PERGAMON

Solid State Communications 119 (2001) 453–458

solid state communications

www.elsevier.com/locate/ssc

Magnetic resonance investigation of the dynamics of F centers in LiF

T. Klempt[a,*], S. Schweizer[b], K. Schwartz[c], O. Kanert[a], D. Suter[a], U. Rogulis[b], J.-M. Spaeth[b]

[a]*Universität Dortmund, Fachbereich Physik, 44221 Dortmund, Germany*
[b]*Universität Paderborn, Fachbereich Physik, 33095 Paderborn, Germany*
[c]*Gesellschaft für Schwerionenforschung, 64291 Darmstadt, Germany*

Received 30 May 2001; accepted 6 June 2001 by P. Dederichs

Abstract

Damage caused in lithium fluoride crystals by γ-rays and electrons includes, besides other point defects, F centers and their agglomerates. We have studied the paramagnetic F centers created by radiation doses that vary by several orders of magnitude. We measured the electronic spin relaxation time T_{1e} of the F centers at low temperatures by the recovery of the magnetic circular dichroism of absorption (MCDA) as well as the temperature dependence of the ^{19}F and ^{7}Li nuclear spin relaxation (NSR) times, T_{1n}. Our results indicate that the nuclear spin relaxation is dominated by spin-diffusion limited paramagnetic relaxation. The electron spin correlation function is determined by the electronic spin–lattice relaxation. In the studied temperature range from 4 to 300 K, the electron spin–lattice relaxation time T_{1e} is long compared to the nuclear Larmor period, $\omega_L T_{1e} \gg 1$ (ω_L: nuclear Larmor frequency). The temperature variation of T_{1n} indicates that the electron spin–lattice relaxation is dominated by phonon-F center interactions. At temperatures T greater than 360 K, an annealing process takes place that eliminates the F centers and their agglomerates.

PACS: 76.60.Es; 76.30.Mi; 61.82.Ms

Keywords: C. Point defects; D. Electron–phonon interactions; D. Spin dynamics; E. Nuclear resonances

1. Introduction

Ionizing radiation in ionic crystals creates a large variety of point defects and related defect clusters. In particular, F centers consisting of an electron in an anion vacancy are a major species among such defects [1,2]. The present paper is focused to the dynamics of F centers in LiF caused by electron and γ irradiation, respectively. The F centers are paramagnetic, and the hyperfine coupling to the neighboring atoms can be measured by EPR [3,4]. Such paramagnetic centers are well known to be a dominant cause of nuclear spin relaxation (NSR) in diamagnetic crystals [5–7]. Bloembergen first introduced the concept of spin diffusion to account for the observed NSR in such materials [5]. A number of solutions of the resulting NSR equation (see Eq. (1)) exist, which depend on the respective boundary conditions in the crystal. The solutions differ from each other concerning the dependence of the NSR rate on the nuclear Larmor frequency, (ω_L), on the concentration of the paramagnetic centers (N_p), and the relaxation time (T_{1e}) of the paramagnetic defects [6]. A large number of studies have been published that dealt with different aspects of NSR induced by paramagnetic defects. For the most part, however, 3d or 4f impurities were used as paramagnetic centers. In the present study, we show that F centers formed, e.g. in LiF by ionizing irradiation, can create a significant NSR for both ^{7}Li and ^{19}F nuclear spins.

2. Nuclear relaxation vs. electronic relaxation

Fluctuations of paramagnetic centers drive nuclear spin polarizations towards thermal equilibrium at a rate that is

* Corresponding author.
E-mail address: thomas@fuj.physik.uni-dortmund.de (T. Klempt).

0038-1098/01/$ - see front matter
PII: S0038-1098(01)00261-7

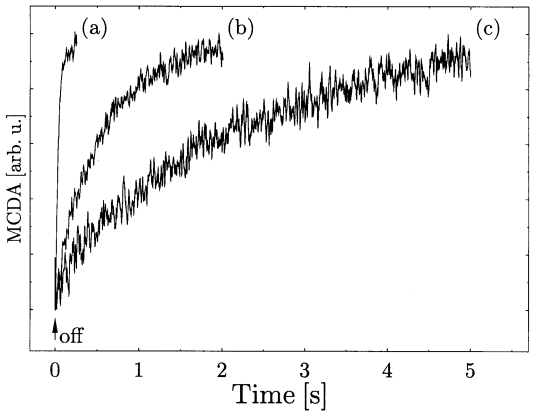

Fig. 1. Time evolution of the F center MCDA in LiF single crystals irradiated by different doses of γ irradiation after switching off the microwaves (25.5 GHz), recorded at 1.5 K, $\lambda = 265$ nm and $B_0 = 930$ mT for γ-doses of (a) 1.122 MGy, (b) 126 kGy, and (c) 1 kGy. All the spectra were normalized to the equilibrium MCDA.

inversely proportional to the sixth power of the distance from this center. The interaction between nuclear spins due to spin diffusion distributes the polarization throughout the crystal. In the vicinity of a paramagnetic center at $r \rightarrow 0$, the combination of these two processes can be written as a differential equation for the density of the nuclear magnetization, $m_z(r,t)$ [6]

$$\frac{\partial m_z}{\partial t} = (m_0 - m_z)Cr^{-6} + D_s\nabla^2 m_z$$
$$\text{with } C = \frac{2}{5}S(S+1)\gamma_e^2\gamma_n^2\hbar^2\frac{T_{1e}}{1+\omega_L^2T_{1e}^2} \quad (1)$$

The first term in Eq. (1) denotes the direct relaxation process due to the dipole–dipole coupling between the F center and the nuclear spins, while the second term describes the transport of magnetization, which is usually called spin diffusion. m_z is the longitudinal nuclear spin magnetization density, m_0 equilibrium magnetization, S the electronic spin, γ_e (γ_n) the gyromagnetic ratio of electronic (nuclear) spin, ω_L the nuclear Larmor frequency, and D_s the spin diffusion coefficient. All the parameters are in the CGS system.

Since the direct relaxation process decreases with the sixth power of the distance from the paramagnetic center, relaxation by spin diffusion dominates at distances larger than $\beta = (C/D_s)^{1/4}$ [6] This distance can be compared to the separation between paramagnetic centers, $R = (3/(4\pi N_p))^{1/3}$, where N_p denotes the concentration of the paramagnetic centers. If $R \gg \beta$, most nuclei interact with the centers only indirectly, and the relaxation process is called 'spin diffusion limited'. The spin diffusion coefficient can be estimated by the relation $D_s \cong a^2/50T_{2n}$ [5], where a is the nearest neighbor distance between like spins and T_{2n} is the spin–spin relaxation time. For LiF, this distance a is 2.85 Å, and $T_{2n} = 8$ μs for ^{19}F and 19 μs for ^{7}Li [8]. The calculated spin diffusion coefficients are $D_s(^{19}\text{F}) = 2\times10^{-12}$ cm^2 s^{-1} and $D_s(^7\text{Li}) = 0.9\times10^{-12}$ cm^2 s^{-1}. In our samples, which were irradiated with γ-rays of a dose of 1–1122 kGy, the values for R were in a range of 5.4×10^{-7}–1.8×10^{-6} cm and those for β, calculated for a magnetic field of 1.22 T and 4.2 K, were in a range of 8.1×10^{-10}–2.3×10^{-9} cm for ^{19}F and 9.8×10^{-10}–2.8×10^{-9} cm for ^{7}Li, respectively; the system should therefore be spin-diffusion limited. If, in addition, the electronic spin relaxation time is slow compared to the nuclear Larmor period, $\omega_L T_{1e} \gg 1$, it is possible to approximate the average nuclear spin relaxation by a single exponential with rate constant [5–7]

$$\frac{1}{T_{1n}} = \frac{8}{3}\pi N_p\left(\frac{2}{5}S(S+1)\gamma_e^2\gamma_n^2\hbar^2\right)^{1/4}\frac{D_s^{3/4}}{\omega_L^{1/2}T_{1e}^{1/4}}. \quad (2)$$

In the following study, we will present independent measurements of the parameters of Eq. (2) and use them to assess the validity of this equation.

3. Experimental

Lithium fluoride has NaCl-structure and a lattice constant of 4.03 Å. These materials also have a band gap of 14 eV (89 nm), therefore the crystal is effectively transparent for optical investigations. F and F_n centers, which are higher aggregated F centers, were created by irradiation with electrons (20 MeV, Dose $D \approx 100$ kGy) or γ-rays from a ^{60}Co source (1.17 and 1.33 MeV, $D = 1$ kGy–5 MGy) at room temperature. The color centers in LiF irradiated with γ-rays and electrons are distributed randomly and correspond to F and F_2 centers and their complementary V centers (absorption at 114 nm in the VUV). Only at doses higher than 1 MGy, the complex color centers (F_n centers with $n \geq 3$) have a noticeable contribution to the absorption in the range of 200–500 nm [1,9]. The irradiated crystals color ranging from yellow through brown to black, depending on the concentration of the defects.

The magnetic circular dichroism of the optical absorption (MCDA), which is the differential absorption of right vs. left circularly polarized light in an external static magnetic field, and the MCDA-detected electron paramagnetic resonance (EPR) were measured in a home-built, computer-controlled spectrometer working at 24 GHz (K-band) at 1.5 K. The MCDA signal is proportional to the population difference of the two electronic spin states of the F center. A resonant microwave field induces EPR transitions, thus changing the relative occupation number of the spin states and thereby the MCDA. The spin–lattice relaxation time T_{1e} is measured by driving the ground state polarization from thermal equilibrium by applying a (saturating) microwave pulse and observing the return of the MCDA to the equilibrium value. The advantage is that the MCDA only depends on the longitudinal magnetization and therefore, only on T_{1e}

Table 1
Doses, F center concentrations, and relaxation times T_{1e} at 1.5 K for γ-irradiated LiF single crystals. The F center concentrations were determined by optical absorption measurements, the relaxation times with the MCDA method

Dose (kGy)	F center concentration (10^{17} cm^{-3})	Relaxation time T_{1e} (s)
1	0.42 ± 0.01	2.3 ± 0.1
10.4	1.96 ± 0.05	4 ± 1
126	6.6 ± 0.2	0.55 ± 0.05
272	8.1 ± 0.2	0.20 ± 0.05
1122	15.3 ± 0.4	0.035 ± 0.005

(for further details see [10]). Examples of such time evolutions are shown in Fig. 1.

The nuclear magnetic resonance (NMR) measurements were carried out with home-built spectrometers with field strengths of 1.22, 4.76 and 8.46 T. The NSR time, T_{1n}, was measured by saturation-recovery pulse sequence. Below 300 K, the temperature was controlled by a flow cryostat (CF1200, Oxford Instruments) regulated by a temperature controller (ITC502, Oxford Instruments). Experiments above room temperature were performed with a home-built probehead and an Eurotherm 2408 temperature controller. Measurements below 1 T were performed with a field-cycling spectrometer.

The LiF crystals are manufactured by Fa. Korth, Kristalle, Germany. The purity of the crystals is about 99.99%, but nothing is known about the kind of the impurities.

4. Results

The F and M centers, which consist of two neighboring F centers, have absorption bands peaking at 245 and 445 nm, respectively. Using an oscillator strength of 0.8, we

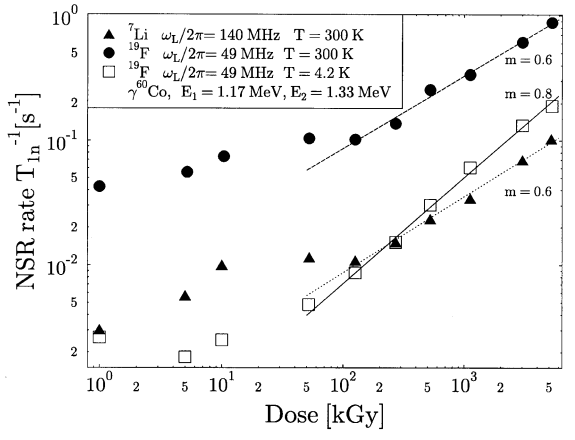

Fig. 2. Dose dependence of the NSR rate of ^{7}Li and ^{19}F. The straight lines indicate a power law with the exponent m.

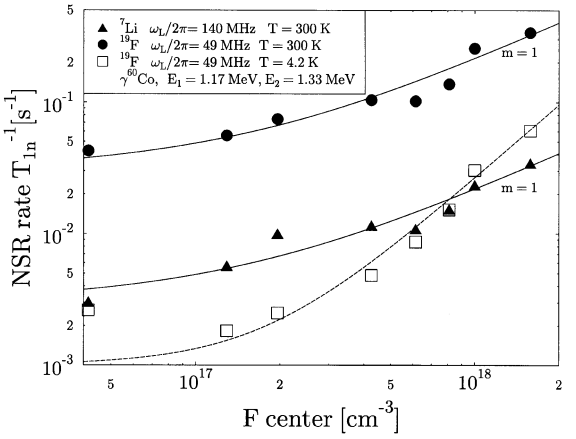

Fig. 3. F center concentration dependence of the NSR rate of ^{7}Li and ^{19}F. The solid and dashed curves fit to the data as dicussed in the text.

determined the concentration of the F centers (N_F) using the Smakula–Dexter formula [9,11]

$$N_F = 9.48 \times 10^{15}\ cm^{-2}\ A/d, \tag{3}$$

where $A = \log(I/I_0)$ denotes the optical absorbance at the band maximum, and d is the thickness of the sample in cm. The calculated concentrations for different radiation doses are listed in Table 1.

The electron spin–lattice relaxation time, T_{1e}, of γ-irradiated crystals was measured by the MCDA method as described in Section 3. The investigated dose ranges was from 1 kGy to 1.122 MGy. Fig. 1 shows the time evolution of the MCDA after a saturating microwave pulse, measured at a wavelength of 265 nm. Comparison of the three time evolutions, corresponding to three doses, shows a rapid increase of the relaxation rate with the F center concentration. The evolution was fitted with a monoexponential decay, and the resulting relaxation times T_{1e} are summarized in Table 1. The faster relaxation at higher doses can be interpreted as a result of increasing interaction between the F centers at higher concentrations [12]. The relaxation time at 10.4 kGy deviates from this trend; the deviation is probably due to a different intrinsic relaxation time in this sample. On the same crystals, we also measured the nuclear spin–lattice relaxation (NSR) times T_{1n}. Fig. 2 shows the dose dependence of the ^{19}F NSR rate at $\omega_L/2\pi$ = 49 MHz (B = 1.22 T) and temperatures of 4.2 and 300 K, and the ^{7}Li NSR rate at $\omega_L/2\pi$ = 140 MHz (B = 8.46 T) and temperature of 300 K. For doses above 126 kGy, the relaxation rate is T_{1n}^{-1} proportional to D^m. Fitted lines, as indicated in Fig. 2 give power law exponents m = 0.6–0.8. At lower doses, the dependence becomes weaker as the relaxation by intrinsic paramagnetic centers starts to dominate the relaxation rate.

Fig. 3 exhibits the dependence of NSR rates on the measured F center concentration N_F. At higher concentrations

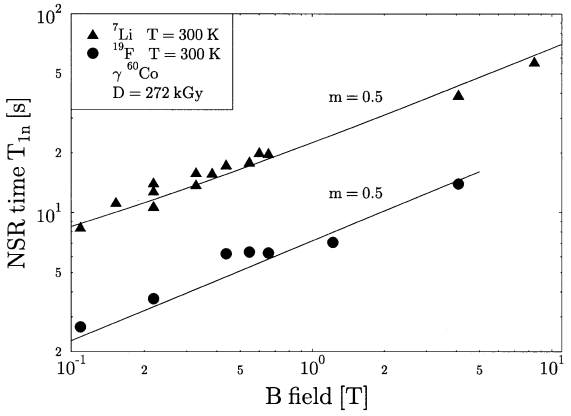

Fig. 4. Magnetic field dependence of the NSR time T_{1n} at room temperature for a γ-dose of 272 kGy from a ^{60}Co decay. The solid lines represent a power law with the exponent $m = 0.5$, as predicted by Eq. (2).

and room temperature, the dependence is linear, as predicted by Eq. (2). Assuming a fixed density (N_0) of intrinsic paramagnetic defects, the data can be described well by $T_{1n}^{-1} = aN_0 + bN_F$ in the entire range of concentration N_F. The solid lines in Fig. 3 confirm the predicted relation using $aN_0 = 0.03,\ 0.003\ s^{-1}$ and $b = 1.9 \times 10^{-19},\ 1.9 \times 10^{-20}\ s^{-1}\ cm^3$ for ^{19}F and ^{7}Li, respectively, as best fit parameters. Unlike the results at room temperature, the NSR data at 4.2 K show a remarkably stronger dependence on N_F. With decreasing temperature the interaction among the F centers becomes more significant which results in a concentration dependence of the related electronic relaxation time, T_{1e} [12]. This is depicted by the measured T_{1e} data listed in Table 1. Hence, according to Eq. (2) and assuming a small density (N_0) one has $T_{1n}^{-1} = aN_0 + cN_F T_{1e}^{-1/4}(N_F)$. The dashed curve in Fig. 3 presents a corresponding fit to the data with $aN_0 = 0.001\ s^{-1}$, $c = 1.6 \times 10^{-20}\ cm^3\ s^{-3/4}$, and $T_{1e}(N_F)$ as given in Table 1. Furthermore, Eq. (2) predicts a magnetic field dependence of the NSR time, T_{1n}. If the electron spin relaxation time does not depend on the field [13], then T_{1n} is proportional to $B^{1/2}$. As depicted in Fig. 4, the prediction is verified experimentally for the sample irradiated with a 272 kGy dose of γ-rays. Based on the experimental results, we were able to compare quantitatively the measured NSR times (T_{1n}) with those calculated by means of Eq. (2) thus confirming the diffusion limited solution of Eq. (1) for F centers in LiF.

As we could not measure the electronic spin relaxation times at 4.2 K, we have extrapolated the 1.5 K data listed in Table 1 by the relation $T_{1e} \propto T^{-1}$, i.e. assuming that a direct process occurs at temperatures below 4 K [14]. For the sample irradiated with 126 kGy γ-rays, one obtains $T_{1e}(4.2\ K) = 196$ ms. The density N_F of the F centers is $6.6 \times 10^{17}\ cm^{-3}$. With $S = 1/2$ and using the observed scaling law $T_{1e} \propto \sqrt{B}$ (see Fig. 4) Eq. (2) predicts $T_{1n}(^{19}F) = 79$ s and $T_{1n}(^7Li) = 144$ s at 4.2 K and $B = 1.22$ T. Table 2 compares these predictions to the experimental data for samples with different concentrations. Considering the approximations inherent in Eq. (2) and the experimental uncertainties, the agreement between the predicted and observed values is good. Hence, it is concluded that Eq. (2) is a good description of the connection between electronic and nuclear relaxation times under the given experimental conditions. This offers the possibility to study the dynamics of the F centers by NSR experiments in a temperature and frequency range that is not directly accessible to ESR measurements.

As one such application, Fig. 5 exhibits the temperature dependence of the ^{19}F NSR rate, T_{1n}^{-1}, for an unirradiated sample (crosses), a sample irradiated with 20 MeV electrons ($D \approx 100$ kGy), and the same sample annealed for 5 min at 473 K. The unirradiated sample shows a rate maximum at 15 K. The NSR in this sample is mostly due to intrinsic paramagnetic centers of unknown origin.The temperature dependent electronic relaxation time, T_{1e}, of these processes at 15 K was obtained from the maximum condition, $\omega_L T_{1e} = 1$. The value of $T_{1e} = 1/\omega_L = 3.2 \times 10^{-9}$ s shows, that the dynamics of the intrinsic centers is extremely fast compared to that of the F centers (see Table 1). The nuclear spin relaxation of the irradiated sample shows a temperature dependence that is roughly linear at low temperature and proportional to the square root of the temperature above 20 K. Around 15 K, the NSR rate is slightly higher; this may originate from the background relaxation observed in the unirradiated sample. As depicted in Fig. 5, however, a very mild annealing (5 min at 473 K) of the irradiated sample significantly changes the temperature dependence of the NSR rate. This results in a distinct

Table 2
Doses, calculated and experimental NSR times of ^{19}F and ^{7}Li in γ-irradiated LiF single crystals. The calculated (according to Eq. (2)) and experimental NSR times were determined for a magnetic field of 1.22 T. The temperature was 4.2 K

Dose (kGy)	^{19}F-T_{1n} calc. (s)	^{19}F-T_{1n} exp. (s)	^{7}Li-T_{1n} calc. (s)	^{7}Li-T_{1n} exp. (s)
1	1750 ± 250	381 ± 4	3200 ± 600	1282 ± 24
10.4	430 ± 70	392 ± 18	790 ± 150	–
126	79 ± 11	115 ± 2	140 ± 20	156 ± 3
272	50 ± 10	66 ± 1	90 ± 20	–
1122	17 ± 3	17 ± 1	31 ± 5	25 ± 1

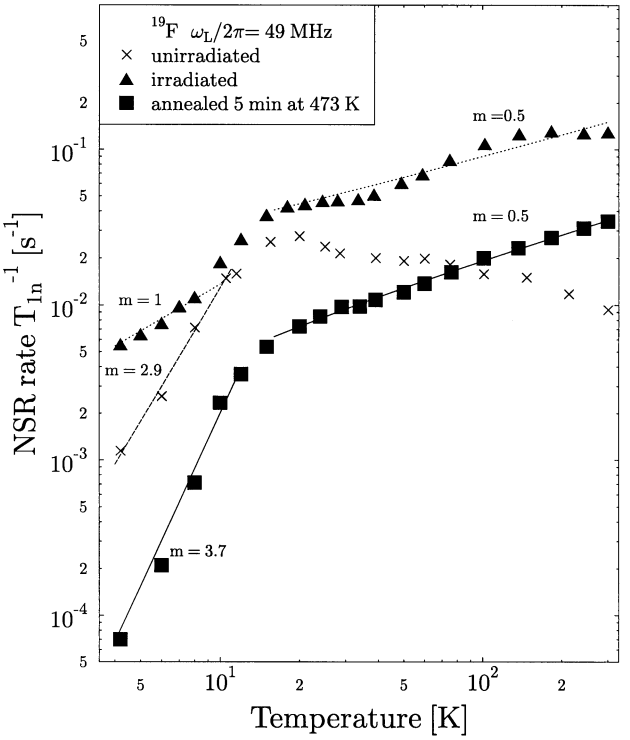

Fig. 5. Temperature dependence of the NSR rate of ^{19}F in LiF single crystals. Crosses: as grown and unirradiated; triangles: irradiated with electrons; squares: irradiated with electrons and annealed for 5 min at 473 K.

temperature dependence of the related NSR rate which can be interpreted by the assumption of a two-phonon induced T_{1e}-process of randomly distributed F centers. At elevated temperatures such a process leads to $T_{1e} \propto 1/T^2$, i.e. according to Eq. (2) $1/T_{1n} \propto T_{1e}^{-1/4} \propto T^{1/2}$ is in good agreement with the experimental findings. At low temperatures, one has $T_{1e} \propto T^n$ with $n = 7$ or 9 depending on the kind of mixing of the Kramers states [14] Then, by use of Eq. (2) one expects $1/T_{1n} \propto T^m$ with $m = 1.75$–2.25 which deviates remarkably from the observed exponent ($m = 3.7$). We suppose that the interaction among the F centers at low temperatures gives rise to the observed enhancement of m, i.e. of the temperature dependence of T_{1e}. The very mild annealing process resulted in an overall reduction of the NSR rate by a factor of four in the high temperature range and a significantly stronger temperature dependence at low temperature. The background contribution visible in the other two samples is largely eliminated in these data. The weaker temperature dependence of the sample with higher F center concentration at lower temperatures can be explained by the theory of Warren, Feldman and Castle [12,14].

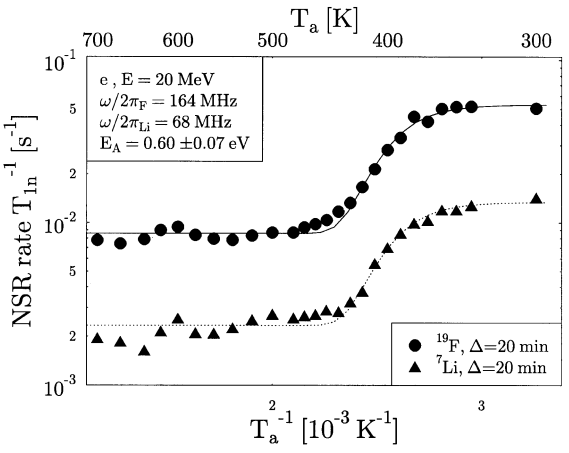

Fig. 6. Stepwise annealing of electron-irradiated samples, measured through the ^{19}F and ^{7}Li NSR rate. Data are fitted by Eq. (6) using the parameters $E_A = 0.60 \pm 0.07$ eV, $T_{1n_{0,1}}(F) = 22.4$ s and $T_{1n_{0,1}}(Li) = 90.5$ s.

If the sample is heated above 360 K, an annealing process sets in that reduces the number of F centers and other defects. We have investigated this process in situ by stepwise annealing, measuring the NSR rate at each step. The temperature of the crystal in the NMR probe was increased to the annealing temperature, T_a, kept there for a time $\Delta = 20$ min, and then cooled down to room temperature, where the NSR rate was measured.

For a thermally activated first order process, we expect

the density N_F of the F centers to change as [15]

$$N_F(t) = -N_F(t)A \exp(-E_A/kT) \quad (4)$$

where E_A is the activation energy and A is a measure of the effectiveness of the process. The solution of the differential equation for an annealing time (Δ) and an annealing temperature (T_a) is:

$$N_F(T_a) = N_{F,0} \exp(-A \exp(-E_A/kT_a)\Delta]. \quad (5)$$

In the experiment, the annealing temperature was raised systematically, and the final density from the last step was the start value for the next step. If the relaxation due to the F centers is proportional to the density of F centers, we expect that the NSR rate after the ith annealing step will be

$$T_{1n,i}^{-1} = T_{1n,i-1}^{-1} \exp[-A \exp(-E_A/kT_{a_i})\Delta] + T_{1n_0}^{-1}, \quad (6)$$

where T_{1n0}^{-1} represents a background relaxation rate that is not affected by the annealing process.

The experimental data (see Fig. 6) are well compatible with this prediction. Fitting the theoretical expression to the experimental data yields an activation energy0 $E_A = 0.60 \pm 0.07$ eV center annealing in LiF for ^{19}F and ^{7}Li data. This value is close to the results on spectroscopic studies of thermal annealing of F centers in LiF irradiated with swift heavy ions [16]. The motion of the F centers seems to be strongly correlated with the diffusion of the Li-ions through the crystal, which has an activation energy of $E_A = 0.65$ eV [17,18]. We can assume, that the movement of the F centers takes place as a movement of the Frenkel pairs.

5. Conclusions

The present work shows that the dynamics of F centers formed by ionizing irradiation (electrons or γ-rays) in LiF is responsible for the observed ^{7}Li and ^{19}F NSR rates. The F center induced NSR process is shown to be treated well by the diffusion-limited solution of Bloembergen's spin-diffusion approach [5] under the condition, $\omega_L T_{1e} \gg 1$, i.e. the relaxation time (T_{1e}) in the entire temperature range is long compared to the nuclear Larmor period. By combining the experimental results of NMR, MCDA and optical absorption, a quantitative confirmation of the diffusion-limited solution (Eq. (2)) could be obtained. Temperature dependent measurements of the ^{19}F NSR rate $1/T_{1n}$ indicate a power law dependence, where $1/T_{1n}$ is proportional to T^m with $m = 1/2$ at elevated temperatures and $m = 3.7$ below 20 K. These findings are compatible with a two-phonon process dominating the relaxation of the F centers. Annealing of the irradiated samples leads to a decrease of both ^{7}Li and ^{19}F NSR rates due to a thermally activated annihilation of the F centers. The corresponding activation energy of the process was found to be $E_A = 0.60 \pm 0.07$eV. In contrast to other investigations of F center in alkali halides, the present study relied strongly on NMR experiments thus demonstrating that NMR is a powerful technique for the investigations of such defects. In a forthcoming paper we will demonstrate that the method can be used successfully also for corresponding studies on extremely non-randomly distributed F centers due to irradiation by heavy ions.

Acknowledgements

We thank Prof. F. Fujara, Dr A. Privalov, O. Lips for access to the field-cycling-spectrometer; Prof. H.J. Weber, H.P. Kreipe for experimental assistance with the optical absorption measurements. The work was supported financially by the Deutsche Forschungsgemeinschaft through the Graduiertenkolleg Festkörperspektroskopie.

References

[1] N. Itoh, M. Stoneham, Materials Modification by Electronic Exitation, Cambridge University Press, Cambridge, 2001.
[2] A.B. Lidiard, Z. Phys. Chem. 206 (1998) 219.
[3] R. Kaplan, P.J. Bray, Phys. Rev. 129 (1963) 1919.
[4] H. Seidel, H.C. Wolf, in: W.B. Fowler (Ed.), Physics of Color Centers, Academic Press, New York, 1968, chapter 8.
[5] N. Bloembergen, Physica 15 (1949) 386.
[6] I.J. Lowe, D. Tse, Phys. Rev. 166 (1968) 279.
[7] W.E. Blumberg, Phys. Rev. 119 (1960) 79.
[8] B.T. Gravely, J.D. Memory, Phys. Rev. B 3 (1971) 3426.
[9] K. Schwartz, C. Trautmann, T. Steckenreiter, O. Geiß, M. Krämer, Phys. Rev. B 58 (1998) 11232.
[10] J.-M. Spaeth, J.R. Niklas, R.H. Bartram, Structual Analysis of Point Defects in Solids, Springer Series in Solid State Science, Vol. 43, Springer, Berlin, 1992.
[11] D.L. Dexter, Phys. Rev. 101 (1956) 48.
[12] R.W. Warren, D.W. Feldman, J.G. Castle Jr., Phys. Rev. A 136 (1964) 1347.
[13] W.E. Blumberg, Phys. Rev. 119 (1960) 1842.
[14] D.W. Feldman, R.W. Warren, J.G. Castle Jr., Phys. Rev. A 135 (1964) 470.
[15] F. Bell, R. Sizmann, Phys. Status Solidi 15 (1966) 369.
[16] C. Trautmann, K. Schwartz, O. Geiss, J. Appl. Phys. Rev. 83 (1998) 3560.
[17] Y. Haven, Rec. Trav. Chim. 69 (1950) 1471.
[18] T.G. Stoebe, R.A. Huggins, J. Mater. Sci. 1 (1966) 117.